# Fine particulate matter promotes airway inflammation and mucin production by activating endoplasmic reticulum stress and the IRE1α/NOD1/NF-κB pathway

LIHUA HU[1,2*], CHAOQUN XU[1,3*], XIANG TANG[1,2], SHANJUN YU[1,2],
LIJUN WANG[1,2], QI LI[1,2] and XIANGDONG ZHOU[1,2]

[1]Department of Respiratory Medicine, The First Affiliated Hospital of Hainan Medical University;
[2]Hainan Province Clinical Medical Center of Respiratory Disease, Haikou, Hainan 570102;
[3]Emergency and Trauma College, Hainan Medical University, Haikou, Hainan 579199, P.R. China

**Abstract.** Fine particulate matter (PM2.5) is a type of small particle that is <2.5 $\mu$m in diameter that may cause airway inflammation. Thus, the present study aimed to explore the effects of PM2.5 on endoplasmic reticulum (ER) stress and airway inflammation in human airway epithelial cells. For this purpose, HBE135-E6E7 airway epithelial cells were cultured and exposed to specific concentrations of PM2.5 for various periods of time, and cell viability was determined using a Cell Counting Kit-8 assay. The results of the present study demonstrated that exposure to PM2.5 increased the mRNA and protein expression levels of interleukin (IL)-6, tumor necrosis factor (TNF)-α and mucin 5AC (MUC5AC). Moreover, the expression levels of ER stress-related proteins, such as glucose-regulated protein 78, CCAAT-enhancer binding protein homologous protein, activating transcription factor 6, protein kinase R-like ER kinase (PERK), phosphorylated (p-)PERK, inositol-requiring enzyme 1α (IRE1α) and p-IRE1α, and nucleotide-binding oligomerization domain 1 (NOD1) expression levels were increased following exposure to PM2.5. Transfection with IRE1α small interfering RNA (siRNA) led to the increased production of IL-6, TNF-α and MUC5AC. Moreover, the expression of NOD1 and the translocation of NF-κB p65 were inhibited following transfection with IRE1α siRNA. In addition, the results of the present study demonstrated that transfection with NOD1 siRNA decreased the production of IL-6, TNF-α and MUC5AC, and decreased the translocation of NF-κB p65. The expression levels of IL-6, TNF-α and MUC5AC were increased in the HBE135-E6E7 cells following treatment with C12-iE-DAP, a NOD1 agonist. Moreover, treatment with C12-iE-DAP led to the activation of NF-κB p65. Collectively, the results of the present study suggest that PM2.5 promotes airway inflammation and mucin production by activating ER stress in HBE135-E6E7 airway epithelial cells, and that the IRE1α/NOD1/NF-κB pathway may be involved in this process.

## Introduction

Fine particulate matter (PM2.5) is a type of small particle with a diameter of <2.5 $\mu$m. PM2.5 is either a solid or liquid particle with the ability to be suspended in air. The results of epidemiological investigations have demonstrated that exposure to PM2.5 is inextricably associated with the development of multiple respiratory diseases, including asthma and chronic obstructive pulmonary disease (COPD), which are exacerbated by airway inflammation and a decline in pulmonary function (1-3). However, the mechanisms by which PM2.5 causes airway inflammation and lung injury are not yet fully understood.

The results of a previous study demonstrated that PM2.5 typically contains a large number of ions, polycyclic aromatic hydrocarbons or lipopolysaccharides, which can induce free radical production, causing reactive oxygen species (ROS) and hydroxyl radical production (4). The overproduction of hydroxyl radicals or ROS may lead to lipid peroxidation of the cell membrane and an elevation in the intracellular calcium concentration, thus disrupting the balance of intracellular calcium homeostasis. In addition, the increase in the intracellular calcium concentration may further enhance the manufacturing of hydroxyl radicals or ROS (5). Notably, the PM2.5-induced accumulation of ROS may play a crucial role in the release of inflammatory mediators and cytokines, such as interleukin (IL)-6 and tumor necrosis factor (TNF)-α, and may induce mucus secretion in the lungs (6). PM2.5-induced lung injury may also cause the hypersecretion

*Correspondence to:* Professor Xiangdong Zhou or Professor Qi Li, Department of Respiratory Medicine, The First Affiliated Hospital of Hainan Medical University, 31 Longhua Road, Longhua, Haikou, Hainan 570102, P.R. China
E-mail: zxd999@263.net
E-mail: lqlq198210@sina.com

*Contributed equally

of various types of mucins, such as mucin 5AC (MUC5AC). The results of previous studies have revealed that MUC5AC levels are increased in the lumen of the endoplasmic reticulum (ER) when airway cells are stimulated by mucus-promoting substances, such as ROS (7,8). Excess mucin and ROS production leads to the accumulation of misfolded proteins in the ER, leading to ER stress (9). Thus, it was hypothesized that ER stress may play a notable role in PM2.5-induced airway inflammation and mucin hypersecretion. Moreover, nuclear factor (NF)-κB plays a key role in ER stress-mediated inflammation (10). There are three major signaling pathways which are associated with ER stress in eukaryotes; namely, inositol-requiring kinase (IRE)1α, protein kinase R-like ER kinase (PERK) and the activating transcription factor (ATF)6 pathways (11). Keestra-Gounder *et al* (12) demonstrated that the nucleotide-binding oligomerization domain (NOD)-like receptor family, including NOD1, activated NF-κB. This activation initiated the gene expression of cytokines and the release of inflammatory factors, which may reveal the association between ER stress and inflammation (12). However, the specific roles of the aforementioned pathways in regulating PM2.5-induced airway inflammation, mucin hypersecretion and ROS overproduction remain to be fully elucidated. Thus, further investigations into the effects of PM2.5 on ER stress and subsequent signaling cascades are required.

The results of a previous study by the authors demonstrated that ER stress may promote airway mucin secretion under the influence of neutrophil elastase (13). Thus, the present study aimed to investigate the effects of ER stress on the management of PM2.5-induced pro-inflammatory factor production, namely ROS and MUC5AC. The present study also aimed to determine the potential pathways involved in PM2.5-induced airway damage. The findings of the present study may provide a basis for the development of novel therapeutic strategies to relieve airway inflammation and mucin hypersecretion.

**Materials and methods**

*Cells, reagents and antibodies.* The immortalized human bronchial epithelial cell line, HBE135-E6E7, was purchased from Procell Life Science & Technology Co., Ltd. The Cell Counting Kit (CCK)-8 (cat. no. E-CK-A362), human MUC5AC enzyme-linked immunosorbent assay (ELISA) kit (cat. no. E-EL-H2279c), Cy3-labeled goat anti-rabbit IgG (cat. no. BA1032) and FITC-labeled goat anti-mouse IgG (cat. no. BA1101) were obtained from Wuhan Boster Biological Technology Co., Ltd. Human IL-6 (cat. no. MM-0049H2) and TNF-α (cat. no. MM-0122H2) ELISA kits were obtained from MMbio. The Annexin V-FITC/PI double staining cell apoptosis detection kit (cat. no. KGA108) was purchased from Nanjing KeyGen Biotech Co., Ltd. Mouse anti-human β-actin monoclonal antibody (cat. no. 66009-1-Ig) was purchased from ProteinTech Group, Inc. Goat anti-rabbit IgG-HRP (cat. no. BA1054) and goat anti-mouse IgG-HRP (cat. no. BA1051) antibodies were purchased from Wuhan Boster Biological Technology, Ltd. Rabbit anti-human glucose-regulated protein 78 (GRP78) polyclonal antibody (cat. no. ab21685), and rabbit anti-human PERK monoclonal antibody (cat. no. ab229912) were obtained from Abcam. Rabbit anti-human phosphorylated (p-)PERK (cat.

no. Bs-3330R) and MUC5AC (cat. no. Bs-7166R) polyclonal antibodies were purchased from BIOSS. Mouse anti-human CCAAT-enhancer binding protein homologous protein (CHOP) monoclonal antibody (cat. no. 2895) was purchased from Cell Signaling Technology, Inc. Mouse anti-human NOD1 monoclonal antibody (cat. no. sc-398696) was purchased from Santa Cruz Biotechnology, Inc. Rabbit anti-human IRE1α (cat. no. DF7709), p-IRE1α (cat. no. AF7150) and ATF6 (cat. no. DF6009) polyclonal antibodies were obtained from Affinity Biosciences. The NF-κB activation-nuclear translocation assay kit (cat. no. SN368) and ROS assay kit (cat. no. C1022) were purchased from the Beyotime Institute of Biotechnology. The ER stress inhibitor, 4-phenylbutyric acid (4-PBA; cat. no. HY-A0281), the ATF6 inhibitor, Ceapin-A7 (cat. no. HY-108434), the PERK inhibitor, ISRIB (cat. no. HY-12495), and the IRE1α inhibitor, 4μ8C (cat. no. HY-19707), were purchased from MedChemExpress. The NOD1 agonist, C12-iE-DAP (cat. no. tlrl-c12dap), was obtained from InvivoGen. Small interfering RNA (siRNA) targeting IRE1α and NOD1, and negative control (NC) siRNA were obtained from GenePharma. The IRE1α siRNA sequence was 5'-GCAGAUAGUCUCUGCCCAUTT-3' (sense), 5'-AUGGGC AGAGACUAUCUGCTT-3' (antisense), the NOD1 siRNA sequence was 5'-CCUUCUUUACAGCCUUCUUTT-3' (sense), 5'-AAGAAGGCUGUAAAGAAGGTT-3' (antisense), and the negative control siRNA sequence was 5'-UUCUCC GAACGUGUCACGUTT-3' (sense), 5'-ACGUGACACGUU CGGAGAATT-3' (antisense).

*Cell viability assay.* The optimal concentration and duration of PM2.5 exposure were determined using a CCK-8 assay, as previously described (14). Briefly, $1x10^4$/ml cells in a 200-μl cell suspension were cultured in a 96-well plate. The cells were subsequently exposed to 10, 50, 100, 200 or 400 μg/ml PM2.5 and cultured at 37˚C in a 5% $CO_2$ environment. Following exposure to PM2.5 for 12, 24 and 48 h, 10 μl CCK-8 were added to each well, and the cells were incubated at 37˚C for a further 2 h. The optical density (OD) was detected using a microplate reader (Multiskan FC; Thermo Fisher Scientific, Inc.) at a wavelength of 450 nm.

*Cell transfection.* Cells were cultured in 24-well plates at a density of $1.5x10^5$/ml with 0.45 ml serum-free RPMI-1640 in each well. To reach a final volume of 50 μl, 5 μl siRNA transfection reagent (Lipofectamine™ 2000; cat. no. 52887; Invitrogen; Thermo Fisher Scientific, Inc.) were mixed with 45 μl serum-free medium. In total, 1 μg aliquots of IRE1α siRNA, NOD1 siRNA or NC siRNA were diluted with 50 μl serum-free medium. Subsequently, the transfection reagent and diluted siRNA were mixed and incubated at room temperature for an additional 20 min. The transfection combination was added to each well drop-by-drop, and vortexed for 10 sec prior to incubation for 16 h at room temperature. The supernatant was removed and the cells were washed three times with phosphate-buffered saline (PBS). The cells were subsequently incubated with fresh RPMI-1640 medium containing 10% fetal bovine serum for 24 h prior to exposure to 100 μg/ml PM2.5.

*Cell culture and grouping.* The HBE135-E6E7 cells were cultured in RPMI-1640 medium at 37˚C in a humidity

Table I. Sequences of primers used in the present study.

| Gene | Primer | Sequence (5'-3') | Accession no. |
|---|---|---|---|
| Homo β-actin | Forward | CCCTGGAGAAGAGCTACGAG | NM_001101.5 |
| | Reverse | CGTACAGGTCTTTGCGGATG | |
| Homo IL-6 | Forward | TTCGGTCCAGTTGCCTTCTCCC | NM_000600.5 |
| | Reverse | CCAGTGCCTCTTTGCTGCTTTC | |
| Homo TNF-α | Forward | CCCATGTTGTAGCAAACCCTC | NM_000594.4 |
| | Reverse | AGAGGACCTGGGAGTAGATGA | |
| Homo MUC5AC | Forward | CTACAATGGACAGCGCTTCC | NM_001304359.2 |
| | Reverse | AGAAGGAGAAGGTGGTTGGG | |

IL-6, interleukin 6; TNF-α, tumor necrosis factor-α; MUC5AC, mucin 5AC.

incubator with 5% $CO_2$. The cells were grouped as follows: i) The control group, in which the cells were cultured under normal conditions (37˚C in a humidity incubator with 5% $CO_2$) with no treatment; ii) the PM2.5 group, in which the cells were exposed to 100 µg/ml PM2.5; iii) the PM2.5 + 4-PBA group, in which the cells treated with 5 mmol/l 4-PBA for 2 h prior to PM2.5 exposure, as previously described (15); iv) the PM2.5 + ISRIB group, in which the cells were treated with 200 nmol/l ISRIB for 2 h prior to PM2.5 exposure, as previously described (16); v) the PM2.5 + Ceapin-A7 group, in which the cells were treated with 20 µmol/l Ceapin-A7 for 2 h prior to PM2.5 exposure, as previously described (17); vi) the PM2.5 + 4µ8C group, in which the cells were treated with 10 µmol/l 4µ8C for 2 h prior to PM2.5 exposure, as previously described (18); vii) the PM2.5 + NC siRNA group, in which the cells were transfected with NC siRNA and subsequently exposed to PM2.5; viii) the PM2.5 + IRE1α siRNA group, in which the cells were transfected with IRE1α siRNA and subsequently exposed to PM2.5; ix) the PM2.5 + NOD1 siRNA group, in which the cells were transfected with NOD1 siRNA and subsequently exposed to PM2.5; and x) the PM2.5 + C12-iE-DAP group, in which cells were treated with 10 µg/ml C12-iE-DAP, as previously described (19), and subsequently exposed to PM2.5. Prior to subsequent experiments, all the cells were incubated at 37˚C for an additional 24 h following grouping.

*Western blot analysis.* Total protein was extracted from the cells using RIPA buffer reagent supplemented with PMSF. Total protein was quantified using a BCA assay and proteins were separated on a 5-10% SDS-PAGE gel; the amount of protein sampled for each sample was 20 µl. The same amount of protein for each sample was subsequently transferred onto PVDF membranes and blocked with PBS containing 0.05% Tween-20 and 5% skimmed milk for 1 h. The membranes were incubated for 2 h at room temperature with primary antibodies against GRP78, CHOP, p-PERK, PERK, ATF6, NOD1, p-IRE1α, IRE1α (dilution for all, 1:500) and β-actin (dilution, 1:1,000). Following washing three times, the membranes were incubated with an HRP-conjugated secondary antibody (dilution, 1:5,000) for 2 h at room temperature. After washing three times, protein bands were visualized using an enhanced chemiluminescence (ECL) reagent (Applygen Technologies

Inc.). Protein expression was quantified using ImageJ software (version 1.8.0; National Institutes of Health) with β-actin as the loading control. The experiment was performed in triplicate, as previously prescribed (20).

*Flow cytometric analysis.* The apoptosis of the HBE135-E6E7 cells was examined using flow cytometry. The cells were inoculated in six-well plates at a density of $3x10^5$ cells per well. The cells were digested with 0.25% trypsin without EDTA, and following the termination of digestion, the treated cells were collected and centrifuged at 800 x g for 5 min at room temperature. The cells were subsequently washed three times with PBS, resuspended in 500 µl binding buffer, and incubated with AV-FITC (5 µl) and PI (5 µl) at room temperature for 15 min in the dark. Apoptotic cells were evaluated using a flow cytometer (cat. no. cytoFLEX; Beckman Coulter, Inc.). The experiment was repeated three times, as previously described (21).

*ELISA.* Cell supernatants were collected following treatment as mentioned above. Various dilutions of cell lysates (1:0, 1:1, 1:2 and 1:5) were treated with PBS, and the expression levels of IL-6, TNF-α and MUC5AC in the cell supernatants were assessed using the corresponding kits, following the manufacturer's protocols. The OD was evaluated using a microplate reader (Multiskan FC; Thermo Fisher Scientific, Inc.) at a wavelength of 450 nm, and the results are presented as percentages of the baseline controls, as previously described (22).

*Reverse transcription-quantitative PCR (RT-qPCR).* Total RNA was extracted from the HBE135-E6E7 cells in each group using TRIzol® reagent (Thermo Fisher Scientific, Inc.), and the RNA samples were incubated at -20˚C for 5 min. The mRNA expression levels of IL-6, TNF-α and MUC5AC were measured using a two-step RT-PCR kit following the manufacturer's protocols (cat. no. R223-01; Nanjing Vazyme Biotech Co., Ltd.). The primer sequences used for PCR (cat. no. Q111-02; Nanjing Vazyme Biotech Co., Ltd.) are displayed in Table I, which were designed using Primer Premier 5.0 software. The following thermocycling conditions were used for qPCR: Initial denaturation at 95˚C for 10 min; 40 cycles of denaturation at 95˚C for 35 sec, annealing at 56˚C for 55 sec and extension at 72˚C for 3 min. The relative

mRNA levels were quantified using the $2^{-\Delta\Delta Cq}$ method (23). All samples were repeated in triplicate.

*Immunofluorescence analysis.* Following treatment as mentioned above, the cells in each group were washed three times with PBS and subsequently fixed with 4% paraformaldehyde at room temperature for 30 min. The cells were washed three times and permeabilized for 15 min with 0.1% Triton X100 (cat. no. ST795; Beyotime Institute of Biotechnology). Subsequently, the cells were blocked with goat serum at room temperature for 45 min, and incubated with antibodies against MUC5AC (dilution, 1:100), NOD1 (dilution, 1:100) or IRE1α (dilution, 1:100) overnight at 4°C. Following three 5-min washes with PBS, the cells were incubated with secondary antibodies labeled with FITC (dilution, 1:100) or Cy3 (dilution, 1:100) for 1 h, and DAPI (cat. no. C1002; Beyotime Institute of Biotechnology) at room temperature for 5 min. The cells were analyzed using a fluorescence microscope (DS-Fi3; Nikon Corporation) to determine the expression of target proteins.

*Assessment of ROS generation.* DCFH-DA (cat. no. S0033; Beyotime Institute of Biotechnology) was diluted in serum-free medium at 1:1,000 to reach a final concentration of 10 µmol/l. Subsequently, the cell culture medium was removed and 10 µmol/l DCFH-DA were added to the cells for incubation at 37°C for 20 min. The cells were then washed three times with serum-free medium to remove the DCFH-DA that was not absorbed by the cells. Images were generated using a fluorescence microscope (DS-Fi3; Nikon Corporation), and ImageJ software (version 1.8.0; National Institutes of Health) was used to assess the fluorescence intensity.

*NF-κB activation-nuclear translocation assay.* Following treatment as mentioned above, the cells were fixed and washed three times with PBS. Subsequently, the cells were blocked with BSA and were then incubated with p65 primary antibody (cat. no. SN368; Beyotime Institute of Biotechnology) (dilution, 1:100) overnight at 4°C. Following three 5-min washes with PBS, the cells were incubated with the secondary antibodies labeled with Cy3 for 1 h. DAPI (dilution, 1:200) at room temperature for 5 min was used to stain the nucleus. The cell supernatants were removed and mounting medium (Jiangsu CITOTEST Scientific Co., Ltd.) was added. Images were generated using a fluorescence microscope (DS-Fi3; Nikon Corporation), and ImageJ software (version 1.8.0; National Institutes of Health) was used to assess the fluorescence intensity, indicative of the levels of NF-κB activation-nuclear translocation.

*Statistical analysis.* All data are presented as the mean ± standard deviation. At least three cell cultures were used in each experiment and repeated in duplicate or triplicate. Multiple groups were compared using one-way ANOVA followed by the Tukey's post hoc test. All data were analyzed using SPSS (version 26.0; IBM Corp.) and R software (version 4.1.2; AT&T Inc.). P<0.05 was considered to indicate a statistically significant difference.

**Results**

*Cell viability following exposure to PM2.5.* To determine the appropriate concentration and duration for exposure to
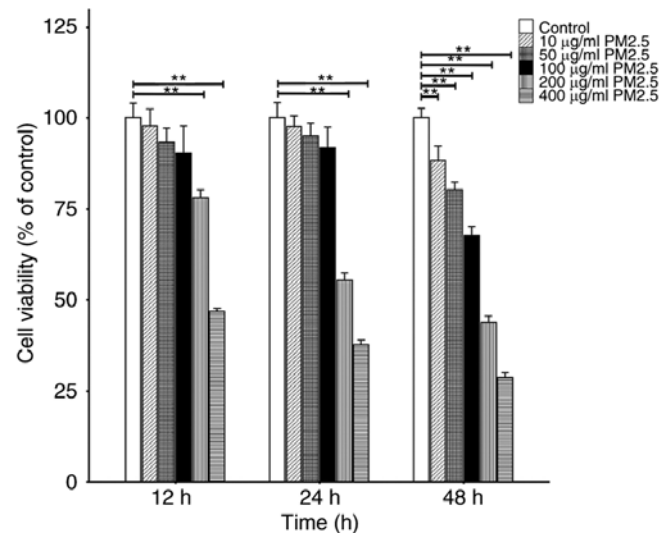


Figure 1. Cell viability assayed using a Cell Counting Kit-8. Cells were exposed to various concentrations of PM2.5 (treatment groups were as follows: Control without PM2.5, and 10, 50, 100, 200 and 400 µg/ml PM2.5) for various periods of time (12, 24 and 48 h). Data are presented as the mean ± SD (n=3 repetitive holes per group). **P<0.01. PM2.5, fine particulate matter.

PM2.5, the cells were exposed to various concentrations (10, 50, 100, 200 and 400 µg/ml) of PM2.5 for specific periods of time (12, 24 and 48 h). Cell viability was determined using a CCK-8 assay. The results demonstrated that the levels of cell viability were comparable from 12 to 24 h between the control group and PM2.5-exposed groups, following exposure to 10-100 µg/ml PM2.5. However, at 12 to 48 h, the levels of cell viability in the groups exposed to 200 and 400 µg/ml PM2.5 decreased compared with the control group, as well as in the 10-100 µg/ml groups at 48 h. Thus, results of the present study suggested that when used for up to 24 h and at 100 µg/ml, PM2.5 did not cause toxicity to the HBE135-E6E7 cells (Fig. 1).

*PM2.5 increases ER stress-related protein expression, which may be reversed by 4-PBA.* To determine whether exposure to PM2.5 activated the ER stress pathway, the expression levels of ER stress-related proteins were detected following exposure to PM2.5. In addition, western blot analysis was carried out to evaluate the protein expression levels of GRP78, CHOP, p-IRE1α, NOD1, ATF6 and p-PERK in the HBE135- E6E7 cells. As illustrated in Fig. 2, exposure to 100 µg/ml PM2.5 for 24 h resulted in increased protein expression levels of GRP78, CHOP, p-IRE1α, NOD1, ATF6 and p-PERK, compared with the control groups. Moreover, the expression levels of these proteins were significantly decreased following pre-treatment with 4-PBA, an ER stress inhibitor, compared with the groups exposed to PM2.5 alone (Fig. 2).

*The IRE1α inhibitor, 4μ8C, exerts suppressive effects on the PM2.5-induced apoptosis of airway epithelial cells.* The results of a previous study demonstrated that ER stress was involved in the apoptosis of various cells (24); however, the effects of the inhibition of ER stress-related pathways on the PM2.5-induced apoptosis of airway epithelial cells remain to be fully elucidated. Thus, herein, the HBE135-E6E7 cells
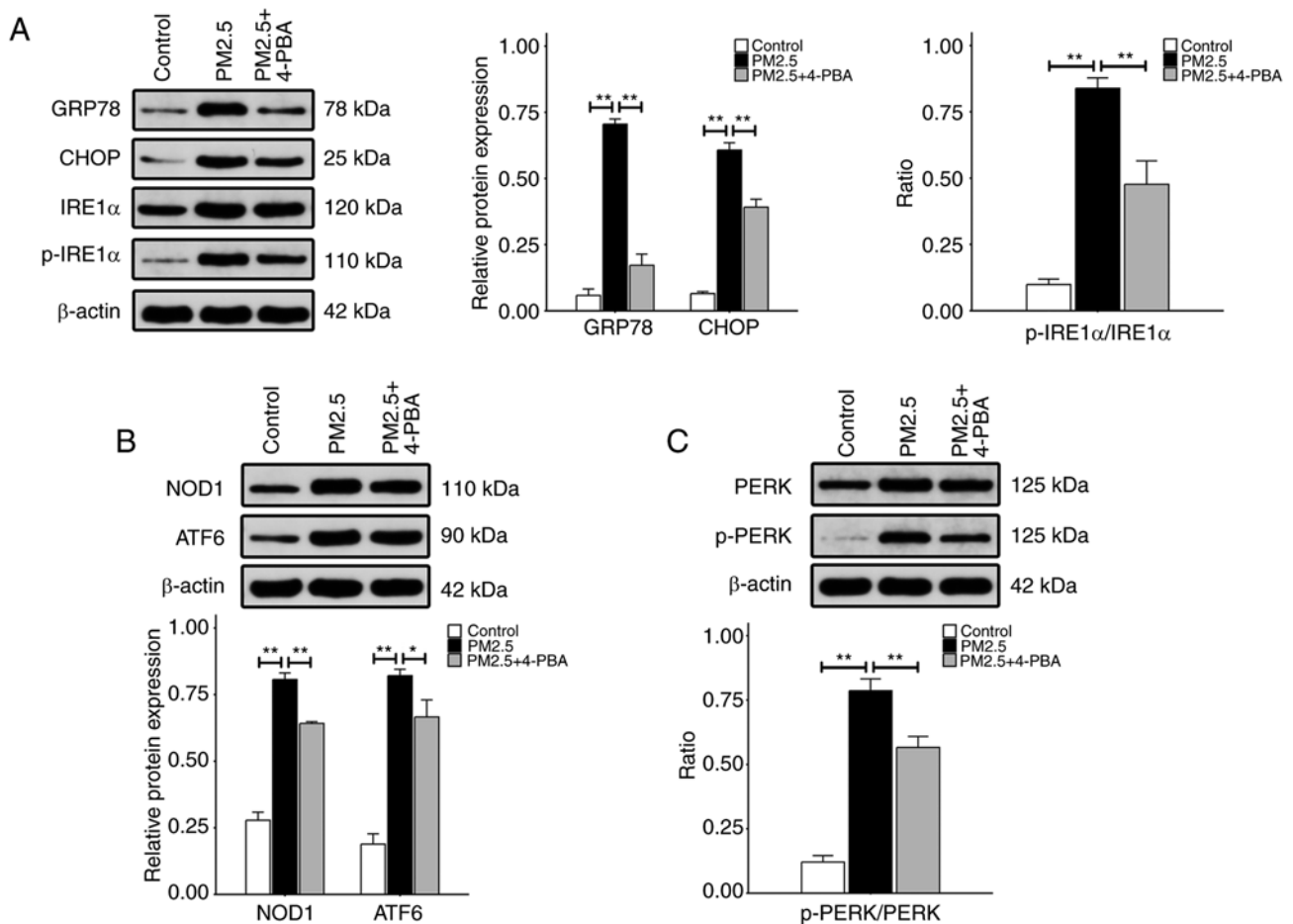
Figure 2. Expression of endoplasmic reticulum stress-related proteins in HBE135-E6E7 cells. Cells were exposed to 100 µg/ml PM2.5, or treated with 5 mmol/l 4-PBA prior to PM2.5 exposure. The levels of the aforementioned proteins were measured using western blot analysis. (A) The relative protein expression levels of GRP78 and CHOP are depicted as the ratio of each to β-actin. The relative p-IRE1α protein expression levels are presented as the ratio of p-IRE1α to IRE1α; β-actin blots were used as the loading control. (B) The same method was used to indicate the relative expression levels of NOD1 and ATF6 proteins. (C) Relative p-PERK protein expression levels. Data are presented as the mean ± SD (n=3 repeats per group). *P<0.05 and **P<0.01. PM2.5, fine particulate matter; 4-PBA, 4-phenylbutyric acid; GRP78, glucose-regulated protein 78; CHOP, CCAAT-enhancer binding protein homologous protein; IRE1α, inositol-requiring kinase 1α; NOD1, nucleotide-binding oligomerization domain 1; ATF6, activating transcription factor 6; PERK, protein kinase R-like endoplasmic reticulum kinase; p-, phosphorylated.

were exposed to 100 µg/ml PM2.5 alone, or treated with 5 mmol/l 4-PBA (an ER stress inhibitor), 200 nmol/l ISRIB (a PERK inhibitor), 20 µmol/l Ceapin-A7 (an ATF6 inhibitor) or 10 µmol/l 4µ8C (an IRE1α inhibitor) prior to exposure to PM2.5. The results of flow cytometric analysis demonstrated that exposure to PM2.5 significantly increased cell apoptosis compared with the control group. However, the effects of PM2.5 exposure were attenuated by the aforementioned ER stress-related inhibitors, compared with PM2.5 exposure alone. Notably, 4µ8C exerted the most potent inhibitory effects on PM2.5-induced apoptosis compared with the other three inhibitors, suggesting that the IRE1α signaling pathway may play a key role in PM2.5-induced airway injury (Fig. 3).

*PM2.5 promotes the production of airway inflammatory cytokines and MUC5AC, which may be mitigated by ER stress-related inhibitors, such as 4µ8C.* To determine the role of ER stress in PM2.5-induced airway inflammation and mucus hypersecretion, the HBE135-E6E7 cells were treated with matched concentrations of PM2.5, 4-PBA, ISRIB, Ceapin-A7 and 4µ8C. The results of ELISA and RT-qPCR assays

demonstrated that PM2.5 significantly promoted the secretion and expression of IL-6, TNF-α and MUC5AC compared with the control groups. However, following pre-treatment with ER stress-related inhibitors, the PM2.5-induced hypersecretion and overexpression of IL-6, TNF-α and MUC5AC were significantly decreased in each group (Fig. 4A-F). The inhibitory effects of 4µ8C pre-treatment on IL-6 secretion were more pronounced than those following 4-PBA or ISRIB pre-treatment (Fig. 4A); however, the inhibitory effects of 4µ8C pre-treatment on IL-6 mRNA expression were only more prominent than those of 4-PBA pre-treatment (Fig. 4D). Compared with the other three inhibitors, 4µ8C inhibited the secretion of TNF-α and MUC5AC at the highest levels (Fig. 4B and C). Moreover, 4µ8C was only superior to 4-PBA in inhibiting the TNF-α mRNA expression levels (Fig. 4E), and was only superior to ISRIB in inhibiting the MUC5AC mRNA expression levels (Fig. 4F). The cell immunofluorescence images of MUC5AC revealed that PM2.5 promoted the intracellular expression of MUC5AC, which was markedly reversed by the four inhibitors mentioned above (Fig. 4G). Collectively, the results of the present study demonstrated that
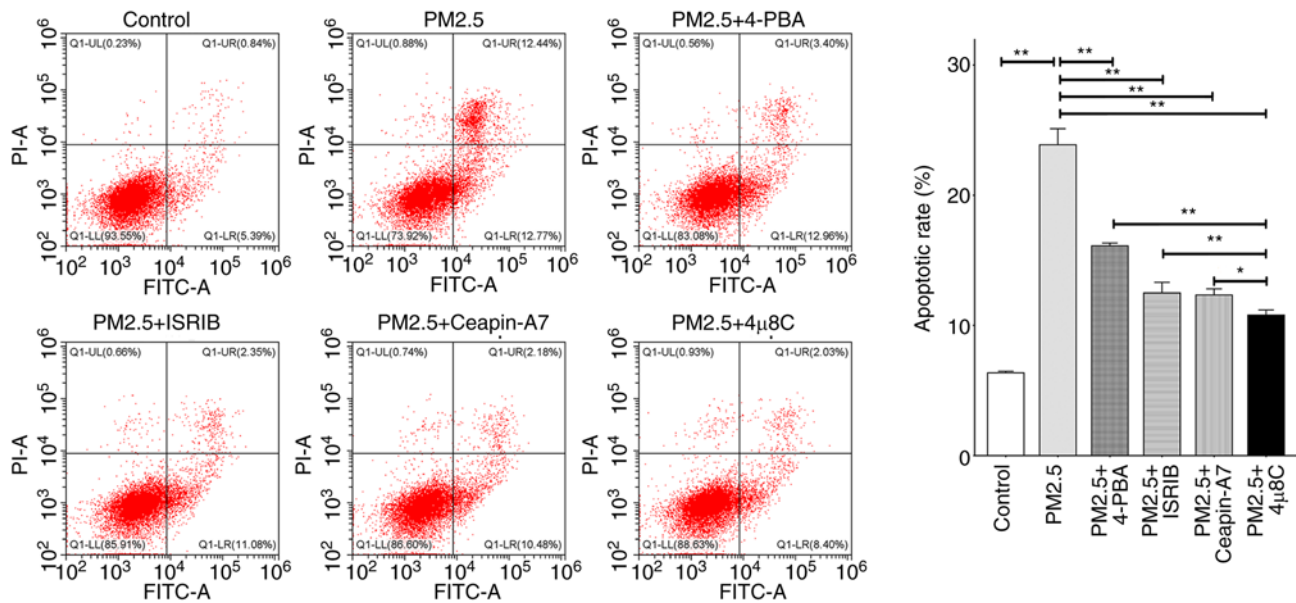
Figure 3. Effects of PM2.5, or pre-treatment with four inhibitors on HBE135-E6E7 cell apoptosis. Cells were pre-treated with 4-PBA (5 mmol/l), ISRIB (200 nmol/l), Ceapin-A7 (20 $\mu$mol/l) and 4$\mu$8C (10 $\mu$mol/l) for 2 h, and then incubated with 100 $\mu$g/ml PM2.5 for 24 h. Flow cytometry was performed to examine apoptosis. All data are presented as the mean ± SD of each group (n=3 repeats per group). *P<0.05 and **P<0.01. PM2.5, fine particulate matter; 4-PBA, 4-phenylbutyric acid; ISRIB, integrated stress response inhibitor.

4$\mu$8C, an IRE1$\alpha$ inhibitor, may exhibit the highest potential in inhibiting PM2.5-induced airway inflammation and mucin hypersecretion.

*Inhibition of ER stress may alleviate the increase of ROS and NF-$\kappa$B induced by PM2.5.* ROS affects several critical aspects of ER stress (25); however, the role of ER stress in the PM2.5-induced overproduction of ROS remains to be fully elucidated. In the present study, the results of DCFH-DA staining demonstrated that ROS production was markedly increased following exposure to PM2.5, and this effect was mitigated following treatment with ER stress inhibitors (Fig. 5A). Notably, the inhibitory effects of 4$\mu$8C on ROS were more pronounced than those of 4-PBA (Fig. 5A); however, there was no significant difference in the inhibitory effects between 4$\mu$8C and ISRIB or Ceapin-A7. In addition, the effects of three ER stress-related pathways (IRE1$\alpha$, ATF6 and PERK) on NF-$\kappa$B activation-nuclear translocation were investigated in the present study. As shown in Fig. 5B, PM2.5 exposure significantly enhanced NF-$\kappa$B activation-nuclear translocation, and this was suppressed by the four ER stress-related inhibitors. Notably, 4$\mu$8C, an IRE1$\alpha$ inhibitor, inhibited NF-$\kappa$B activation-nuclear translocation at a higher level than ISRIB (a PERK inhibitor), Ceapin-A7 (an ATF6 inhibitor) and 4-PBA (an ER stress inhibitor). These results demonstrated that IRE1$\alpha$ may play a key role in the regulation of NF-$\kappa$B activation.

*IRE1$\alpha$ regulates NF-$\kappa$B via NOD1 in PM2.5-induced ER stress.* The results of the present study demonstrated that IRE1$\alpha$ exhibited the highest potential in the PM2.5-induced regulation of ER stress and NF-$\kappa$B; however, the potential signaling cascades of IRE1$\alpha$ remain unclear. NOD1, a newly discovered ER stress-related protein, may interact with IRE1$\alpha$. Firstly, the inhibition efficiency of IRE1$\alpha$ siRNA, NOD1

siRNA, or NC siRNA was evaluated using RT-qPCR and it was found that compared with control groups, no change in IRE1$\alpha$ or NOD1 mRNA levels was observed when the HBE135-E6E7 cells were transfected with NC siRNA alone; however, there was a significant decrease in the mRNA levels of IRE1$\alpha$ or NOD1 following transfection with IRE1$\alpha$ siRNA or NOD1 siRNA alone, and the inhibitory efficiencies reached ~70% in both cases (Fig. 6A and B). The cells were then transfected with IRE1$\alpha$ siRNA, NOD1 siRNA or NC siRNA prior to exposure to 100 $\mu$g/ml PM2.5. As shown in Fig. 6C, the results of western blot analysis demonstrated that exposure to PM2.5 promoted the expression of p-IRE1$\alpha$, and this was not affected by prior transfection with NC siRNA. In addition, p-IRE1$\alpha$ was significantly inhibited following transfection with IRE1$\alpha$ siRNA. Notably, results of the western blot analysis were comparable with the immunofluorescence intensity of IRE$\alpha$ in each group (Fig. 6D). These results indicated that IRE1$\alpha$ siRNA inhibited the expression and phosphorylation of IRE1$\alpha$. As shown in Fig. 6E, PM2.5 exposure significantly increased the protein expression levels of NOD1, compared with the control group. There was no significant difference in NOD1 expression between the PM2.5 + NC siRNA and PM2.5 groups. However, pre-treatment with IRE1$\alpha$ siRNA markedly reduced the PM2.5-induced increase in NOD1 expression, indicating that IRE1$\alpha$ modulates NOD1 in PM2.5-induced ER stress. In addition, NOD1 expression was markedly decreased in the PM2.5 + NOD1 siRNA group compared with the PM2.5 group, suggesting that NOD1 siRNA inhibited the expression of NOD1. Moreover, following pre-treatment with C12-iE-DAP, a NOD1 agonist, there was a significant increase in NOD1 expression compared with the PM2.5 group. Similar results were obtained using immunofluorescence analysis (Fig. 6F). In addition, the effects of pre-treatment with IRE1$\alpha$ siRNA or NOD1 siRNA on the PM2.5-induced NF-$\kappa$B activation-nuclear translocation were then investigated. As shown in Fig. 6G,
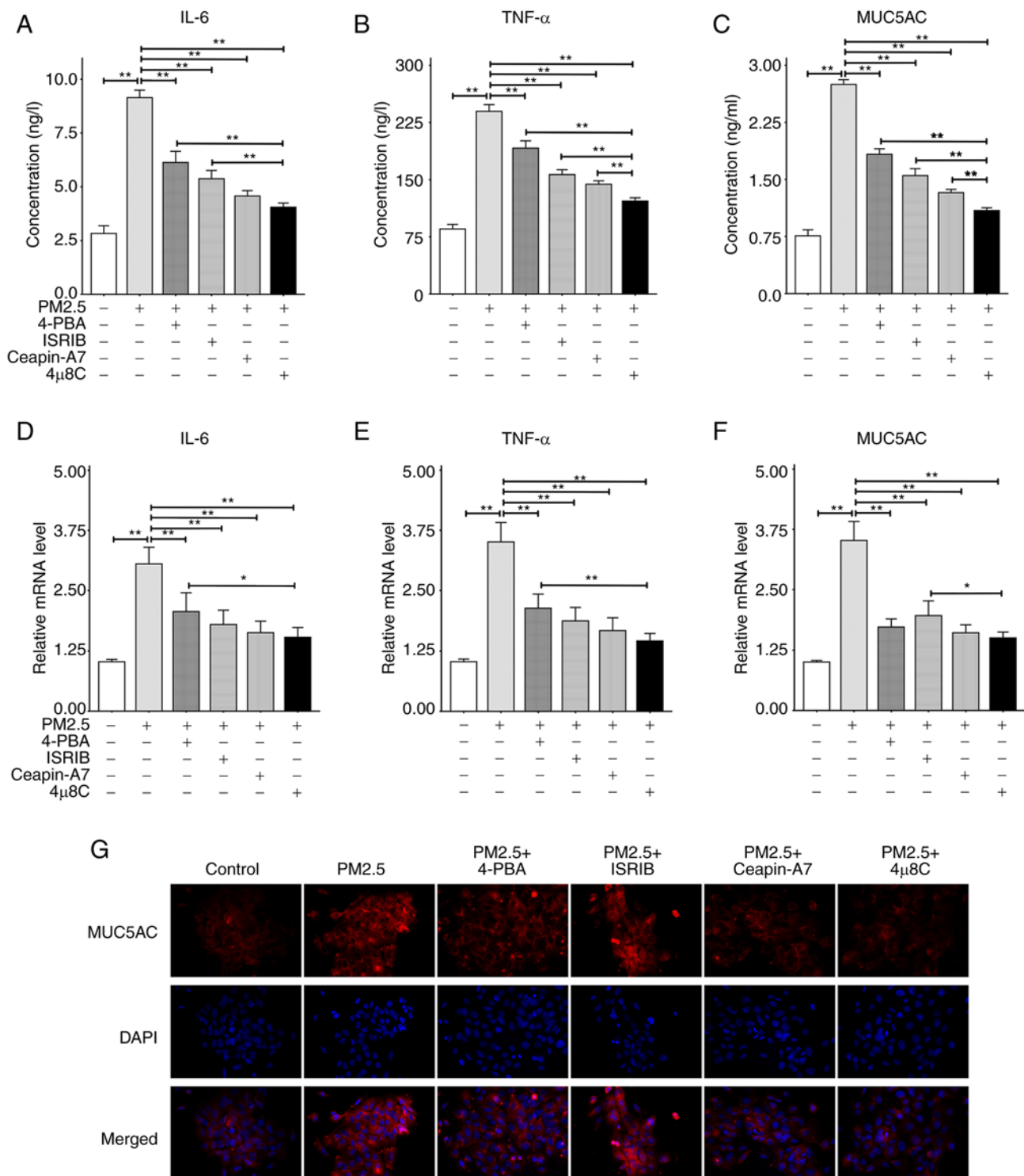
Figure 4. Secretion and mRNA expression levels of IL-6, TNF-α and MUC5AC. ELISA was used to detect the levels of inflammatory factors and mucin secretion. RT-qPCR assay was utilized to measure the mRNA expression level of the target protein relative to β-actin. Cells were pre-treated with 4-PBA (5 mmol/l), ISRIB (200 nmol/l), Ceapin-A7 (20 $\mu$mol/l) and 4$\mu$8C (10 $\mu$mol/l) for 2 h, and then incubated with 100 $\mu$g/ml PM2.5 for 24 h. (A) ELISA results of IL-6. (B) ELISA results of TNF-α. (C) ELISA results of MUC5AC. (D) RT-qPCR results of IL-6. (E) RT-qPCR results of TNF-α. (F) RT-qPCR results of MUC5AC. (G) Intracellular expression of MUC5AC detected using immunofluorescence at x400 magnification. All data are presented as the mean ± SD of each group (ELISA and RT-qPCR with n=3 repeatsper group, and immunofluorescence with n=3 different field images per group). *P<0.05 and **P<0.01. PM2.5, fine particulate matter; IL-6, interleukin-6; TNF-α, tumor necrosis factor-α; MUC5AC, mucin 5AC; 4-PBA, 4-phenylbutyric acid; ISRIB, integrated stress response inhibitor; RT-qPCR, reverse transcription-quantitative PCR.

there was a notable decrease in the activation-nuclear translocation of NF-κB in the PM2.5 + IRE1α siRNA or PM2.5 + NOD1 siRNA groups, compared with the PM2.5 + NC siRNA group. However, pre-treatment with C12-iE-DAP further increased the NF-κB activation-nuclear translocation induced by PM2.5. These results suggested that in PM2.5-induced ER stress, IRE1α may promote the NF-κB activation-nuclear translocation by increasing the expression of NOD1.
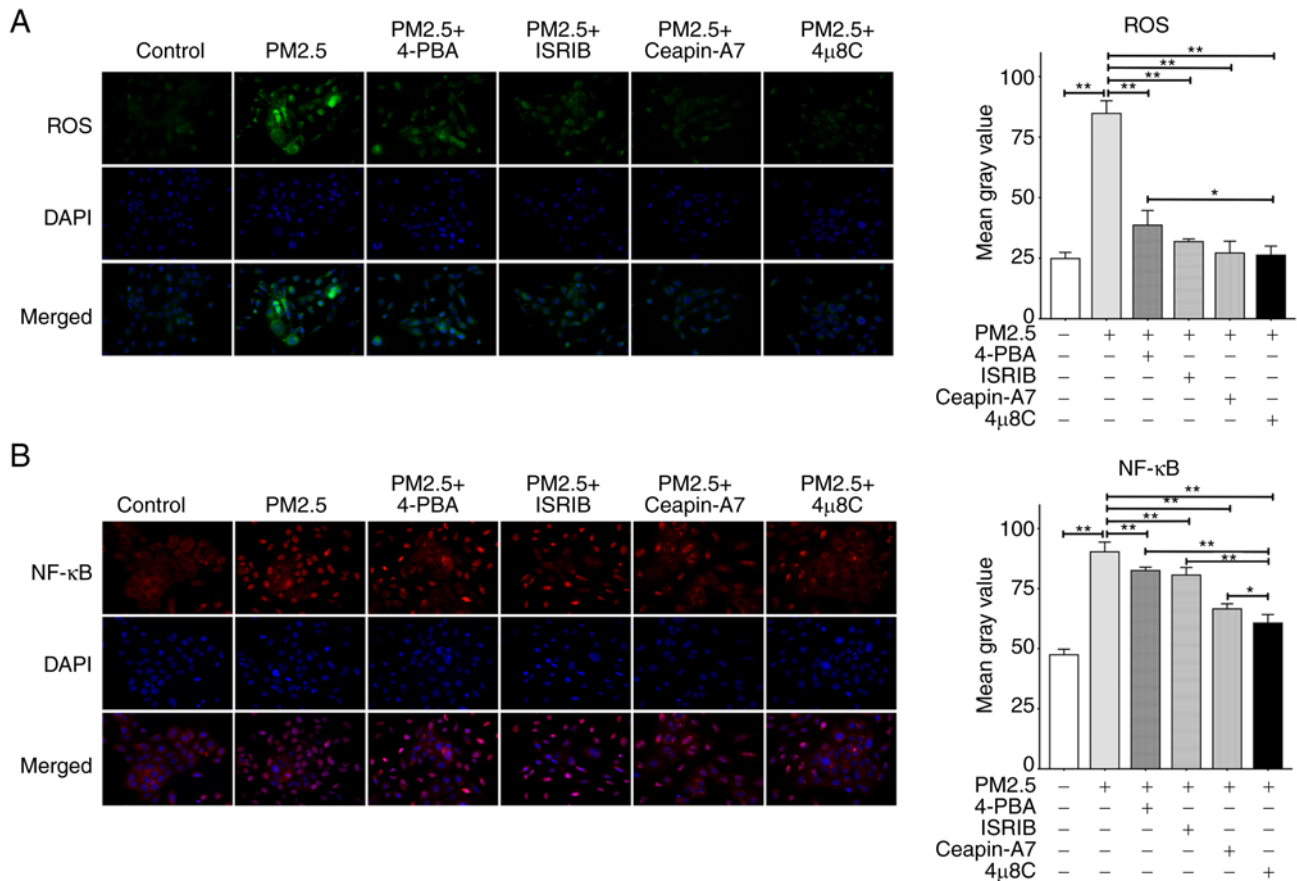
Figure 5. (A) The intracellular ROS generation was determined using DCFH-DA. (B) The intracellular NF-κB activation-nuclear translocation was assayed using a specialized kit. All images were detected using a fluorescence microscope at x400 magnification, and the mean gray values were computed using ImageJ software. Data are presented as the mean ± SD (n=3 different field images per group). *P<0.05 and **P<0.01. PM2.5, fine particulate matter; ROS, reactive oxygen species; 4-PBA, 4-phenylbutyric acid; ISRIB, integrated stress response inhibitor.

*PM2.5 promotes airway inflammation and mucin production through the IRE1α/NOD1/NF-κB pathway*. The results of the present study demonstrated that the expression levels of IL-6, TNF-α, MUC5AC, IRE1α and NOD1 were increased following PM2.5 exposure, and IRE1α regulated the activation-nuclear translocation of NF-κB via NOD1. The results of previous studies have demonstrated that NF-κB plays a critical role in regulating airway inflammation and mucus hypersecretion (26,27). Therefore, herein, the effects of the IRE1α/NOD1/NF-κB pathway on the expression of inflammatory cytokines and mucin were investigated following exposure to PM2.5. As illustrated in Fig. 7A-F, there was a notable decrease in the secretion and mRNA expression of IL-6, TNF-α and MUC5AC compared with the PM2.5 + NC siRNA group, regardless of IRE1α siRNA or NOD1 siRNA pre-treatment. However, following pre-treatment with C12-iE-DAP, the secretion and mRNA expression of IL-6, TNF-α and MUC5AC were significantly increased. The results of the immunofluorescence analysis demonstrated that MUC5AC was markedly attenuated in the PM2.5 + IRE1α siRNA and PM2.5 + NOD1 siRNA groups, compared with the PM2.5 + NC siRNA group. In addition, the fluorescence intensity was markedly increased in the PM2.5 + C12-iE-DAP group (Fig. 7G), and these results were comparable with those obtained using ELISA and RT-qPCR (Fig. 7A-F). These results suggested that PM2.5 may promote the expression of

IREα, NOD1 and NF-κB activation-nuclear translocation, thus, promoting airway inflammation and mucin production.

## Discussion

The findings of the present study demonstrated that PM2.5 activated ER stress-related proteins, including CHOP, GRP78, ATF6, PERK, p-PERK, IRE1α, p-IRE1α and NOD1. These proteins enhanced the apoptosis of airway epithelial cells, resulting in an increase in the levels of ROS, IL-6, TNF-α and MUC5AC. These increases were significantly alleviated following pre-treatment with ER stress-related inhibitors, such as 4-PBA, ISRIB, Ceapin-A7 and 4μ8C. Moreover, the results of the present study demonstrated that transfection with IRE1α siRNA reduced NOD1, NF-κB, IL-6, TNF-α and MUC5AC expression, and transfection with NOD1 siRNA also decreased NF-κB, IL-6, TNF-α and MUC5AC expression. C12-iE-DAP treatment increased the levels of NOD1, NF-κB, IL-6, TNF-α and MUC5AC, suggesting that the IREα-induced promotion of NOD1 increased NF-κB, which may play a role in the overproduction of inflammatory cytokines and mucin induced by PM2.5.

The results of a previous study demonstrated that various particles induce tissue necrosis and cell apoptosis, followed by the release of intracellular contents. This may include the release of non-zyme lactate dehydrogenase, which is
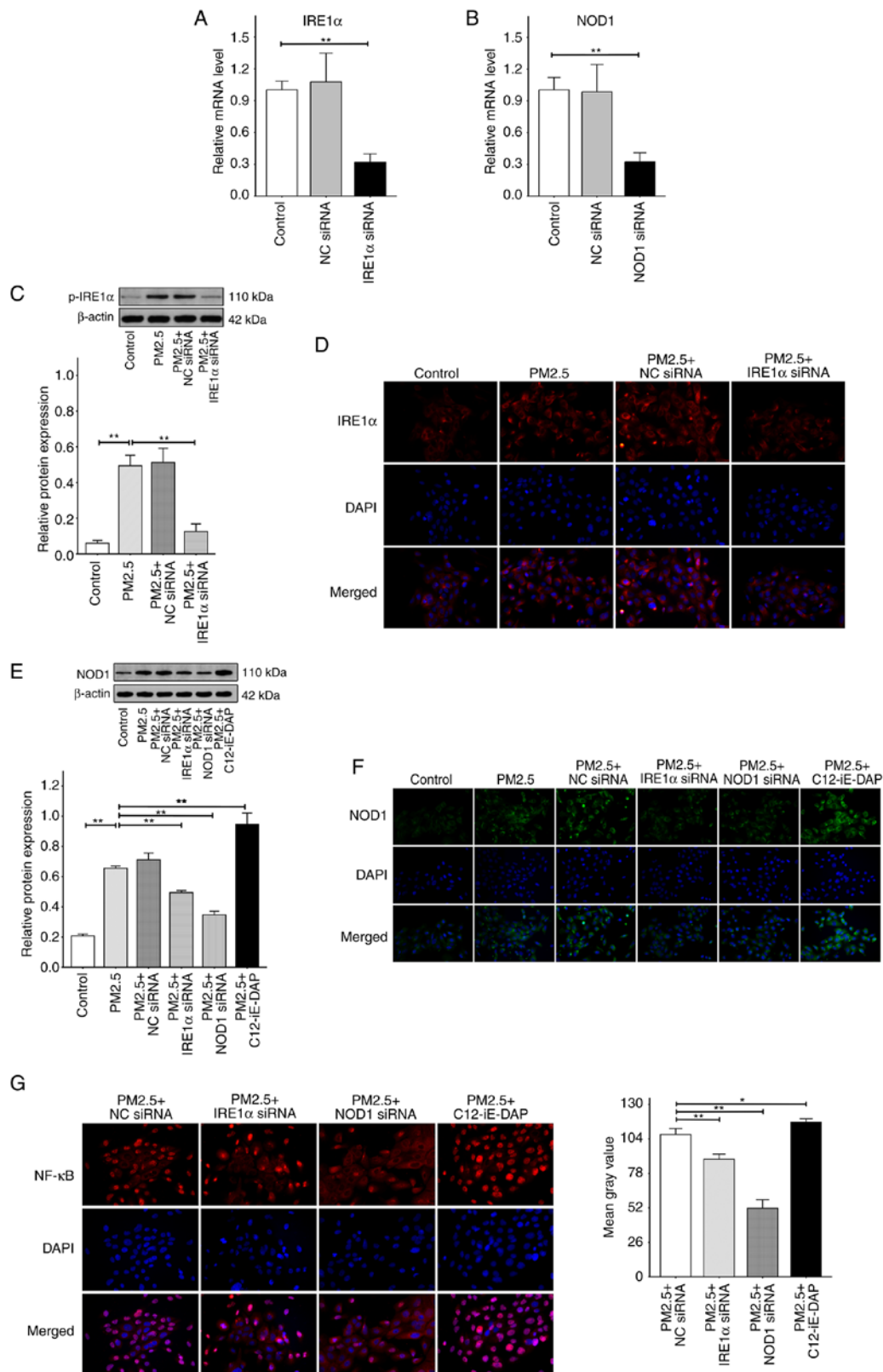
Figure 6. The levels of p-IRE1α, IRE1α and NOD1 expression, and NF-κB activation-nuclear translocation. The cells were transfected with negative control (NC) siRNA, IRE1α siRNA or NOD1 siRNA respectively, or were pretreated with 10 μg/ml C12-iE-DAP (a NOD1 agonist) for 2 h prior to exposure to 100 μg/ml PM2.5 for 24 h. (A) The mRNA expression levels of IRE1α relative to β-actin measured by RT-qPCR. (B) The mRNA levels of NOD1 relative to β-actin. (C) Relative protein expression levels of p-IRE1α, detected by western blot, were depicted as the ratio of each group to β-actin. (D) The expression levels of IRE1α, assayed by the immunofluorescence labeled by CY3, were detected using a fluorescence microscope at x400 magnification. (E) Relative protein expression levels of NOD1, detected using western blot analysis. (F) The expression levels of NOD1, assayed using immunofluorescence labeled with FITC, were detected using a fluorescence microscope at x400 magnification. (G) The intracellular NF-κB activation-nuclear translocation, assayed using a specialized kit, were also detected using a fluorescence microscope at x400 magnification, and the mean gray values were computed using ImageJ software. Data are presented as the mean ± SD (RT-qPCR and western blot with n=3 repeats per group, and immunofluorescence with n=3 different field images per group). *P<0.05 and **P<0.01. RT-qPCR, reverse transcription-quantitative PCR; PM2.5, fine particulate matter; IRE1α, inositol-requiring kinase 1α; NOD1, nucleotide-binding oligomerization domain 1.
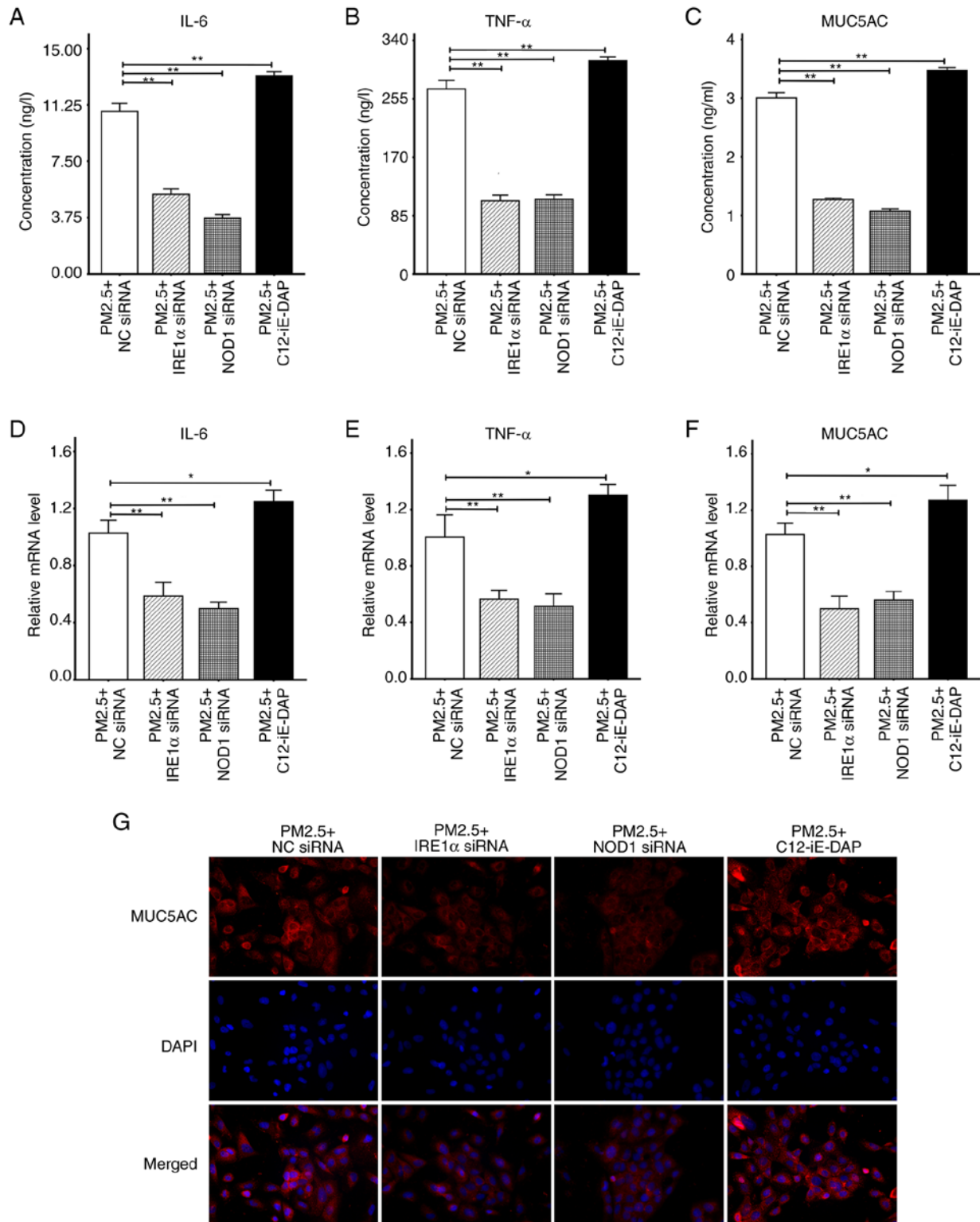
Figure 7. (A) The secretion levels of IL-6. (B) The secretion levels of TNF-α. (C) The secretion levels of MUC5AC. (D) The mRNA expression levels of IL-6. (E) The mRNA expression levels of TNF-α. (F) The mRNA expression levels of MUC5AC. (G) The intracellular MUC5AC expression determined by immunofluorescence microscope at 400x magnification. The secretion levels of IL-6, TNF-α and MUC5AC were detected by ELISA. The mRNA expression levels of IL-6, TNF-α and MUC5AC relative to β-actin were measured by RT-qPCR. Cells were transfected with negative control (NC) siRNA, IRE1α siRNA or NOD1 siRNA, or were pre-treated with 10 $\mu$g/ml C12-iE-DAP (a NOD1 agonist) for 2 h prior to exposure to 100 $\mu$g/ml PM2.5 for 24 h. Data are presented as the mean ± SD (ELISA and RT-qPCR with n=3 repeats per group, and immunofluorescence with n=3 images per group). $^*P<0.05$ and $^{**}P<0.01$. PM2.5, fine particulate matter; MUC5AC, mucin 5AC; IRE1α, inositol-requiring kinase 1α; NOD1, nucleotide-binding oligomerization domain 1.

associated with the release of free radicals (28). Subsequently, the release of intracellular contents may lead to the recruitment of inflammatory cells, such as macrophages, monocytes

and natural killer cells. These cells may secrete TNF-α, which is associated with inflammation in various processes (29). PM2.5 is often generated via the burning of coal and diesel

engine exhaust emissions. As the aerodynamic diameter of PM2.5 is <2.5 $\mu$m (30), a higher proportion of the particles are deposited in the lungs where they permeate deep alveoli, thus, affecting the respiratory system and potentially entering the bloodstream (31). PM2.5 also promotes airway oxidative stress, inflammation and mucin hypersecretion, which may cause long-term airway damage. At present, research is focused on determining the effects of PM2.5 on respiratory diseases, such as asthma and COPD. However, the effectiveness of current treatment options for PM2.5 remain limited, and further investigations are required to determine the mechanisms responsible for PM2.5-induced airway damage.

Previous studies have demonstrated that the ER stress response is a fundamental characteristic in numerous inflammatory diseases, and this may activate the unfolded protein response (UPR) (32,33). UPR performs an adaptive role in protein quality assurance to promote optimal protein synthesis, secretion and folding in ER to reverse ER stress (34). In addition, ER stress is involved in various airway inflammatory diseases, including lung infections, pulmonary fibrosis, asthma and COPD (33,35). However, the specific role of ER stress in PM2.5-induced airway injury is not yet fully understood. Molagoda *et al* (36) reported that the inhibition of ER stress protected HaCaT human keratinocytes from PM2.5-induced oxidative stress and apoptosis (36), and similar results were observed in the present study using HBE135-E6E7 airway epithelial cells. Kim *et al* (37) revealed that the inhibition of ER stress alleviated the lipopolysaccharide-induced production of inflammatory cytokines in healthy human bronchial epithelial cells (37), which was also consistent with the results of the present study. The results of previous studies have also confirmed that ER stress may be involved in the hypersecretion of airway mucin (38,39). Notably, the role of ER stress in PM2.5-induced mucin hypersecretion was demonstrated in the present study. In summary, ER stress may play a key role in PM2.5-induced airway injury; however, further investigations into the specific underlying mechanisms are required.

As ER transmembrane receptors, ATF6, PERK and IRE1 are considered the three major signaling pathways in maintaining ER homeostasis, and function differently in the pathogeneses of various airway diseases (40-42). On the one hand, p-PERK promotes the phosphorylation of eukaryotic translation initiation factor 2$\alpha$ (eIF2$\alpha$), inhibiting the transcription of numerous proteins. On the other hand, IRE1 and ATF6 may localize in the nucleus and enhance the transcription of UPR chaperone proteins, such as GRP78, to enhance folding capacity and decimate misfolded proteins for relieving ER stress (43). As previously demonstrated, in a PM2.5-exposed macrophage cell line, UPR was mediated by the PERK-eIF2$\alpha$ axis (44). However, in human airway epithelial cells, IRE1 and ATF6 play a major role in mucin hypersecretion (7,13). These results suggest that the importance of the three aforementioned ER stress-related signaling pathways may vary under different conditions. Notably, IRE1 exists in two isoforms; namely, IRE1$\alpha$ and IRE1$\beta$. IRE1$\alpha$ may be expressed in numerous cell types; however, IRE1$\beta$ is restricted to epithelial cells, mainly in the gastrointestinal tract (45). The present study demonstrated that 4$\mu$8C, only inhibiting one of the pathways in the process of ER stress, had a more potent inhibitory effect than 4-PBA inhibiting ER stress as a whole. The reason for this result may

be that 4$\mu$8C inhibits only one pathway of ER stress, which is more targeted and specific compared to 4-PBA. The inhibition of three pathways by 4-PBA may result in a weak inhibitory effect on each pathway. The IRE1$\alpha$ pathway may be more crucial in promoting PM2.5-induced ER stress. The results of a previous study confirmed that IRE1$\alpha$ promoted NF-$\kappa$B by increasing X-box-binding protein 1, which plays a key role in the inflammatory response of airway epithelial cells (46). The results of the present study demonstrated that ATF6, PERK and IRE1$\alpha$ exert specific regulatory effects on PM2.5-induced apoptosis and the overproduction of ROS, IL-6, TNF-$\alpha$ and MUC5AC; however, IRE1$\alpha$ exhibited a greater regulatory potential. Moreover, in homeostatic states, GRP78 is attached to the specific domains of ATF6, PERK and IRE1$\alpha$ to prevent them from activation. Under conditions of stress, GRP78 is redirected to unfolded proteins of the ER, activating the three transducers (47). In addition, CHOP controls the intricate interaction between the adaptive and apoptotic branches of the UPR (48). Therefore, both GRP78 and CHOP exhibit potential as ER stress markers. Collectively, the results of previous studies and those of the present study indicated that GRP78 and CHOP may be elevated in the airway under the influence of various stimuli, including ovalbumin, lipopolysaccharide, house dust mites or PM2.5 (49,50).

Among the multitudinous airway cells, epithelial cells serve as a physical barrier between the body and the external environment, and activate the inflammatory response to external stimuli (51). Epithelial cells express numerous pattern recognition receptors, including Toll-like receptors (TLRs), NOD1 and NOD2, to identify different external triggers, producing chemokines and cytokines (52). A previous study demonstrated that IRE1$\alpha$ activated TLR2, TLR4 and NF-$\kappa$B for involvement in ER stress caused by bacteria and mycobacteria (53). Notably, the results of a previous study demonstrated that NOD1 and NOD2, which play roles in detecting bacterial peptidoglycan, may also transduce ER stress signals to trigger inflammation (54). Keestra-Gounder *et al* (12) demonstrated that IRE1$\alpha$ activation promoted NOD1 and NOD2 to mediate the inflammatory branch of the UPR. The present study further demonstrated that PM2.5 activated IRE$\alpha$, promoted NOD1 and enhanced NF-$\kappa$B to overproduce airway inflammation and mucin. However, further studies are required to focus on further verifying the effects of ER stress on ROS, inflammatory factors and mucin production, and determine the regulatory role of the IRE1$\alpha$/NOD1/NF-$\kappa$B pathway in animal models of PM2.5-induced lung injury. Moreover, further investigations into the mutual promotion mechanism between IRE1$\alpha$ and NOD1 in ER stress are warranted.

In conclusion, the results of the present study suggested that ER stress was involved in PM2.5-induced apoptosis, and the overproduction of ROS, inflammatory cytokines and mucin in airway epithelial cells. Furthermore, the IRE1$\alpha$/NOD1/NF-$\kappa$B pathway may play a critical role in airway inflammation and mucin hypersecretion caused by PM2.5. Blocking the IRE1$\alpha$/NOD1/NF-$\kappa$B pathway may exhibit potential in the treatment of airway damage.

## Acknowledgements

## Availability of data and materials

The datasets used and/or analyzed during the current study are available from the corresponding author on reasonable request.

## Authors' contributions

LH and CX obtained and evaluated the data, and wrote the final manuscript. XT, SY and LW carried out the cell experiments. QL and XZ designed and conceptualized the study. XZ carefully reviewed this manuscript and managed the progress of the experiments. LH, CX, QL and XZ confirm the authenticity of all the raw data. All authors have read and agreed with the final version of the manuscript.

## Ethics approval and consent to participate

Not applicable.

## Patient consent for publication

Not applicable.

## Competing interests

The authors declare that they have no competing interests.

## References

1. Gleason JA, Bielory L and Fagliano JA: Associations between ozone, PM2.5, and four pollen types on emergency department pediatric asthma events during the warm season in New Jersey: A case-crossover study. Environ Res 132: 421-429, 2014.
2. Montoya-Estrada A, Torres-Ramos YD, Flores-Pliego A, Ramirez-Venegas A, Ceballos-Reyes GM, Guzman-Grenfell AM and Hicks JJ: Urban PM2.5 activates GAPDH and induces RBC damage in COPD patients. Front Biosci (Schol Ed) 5: 638-649, 2013.
3. Davel AP, Lemos M, Pastro LM, Pedro SC, de André PA, Hebeda C, Farsky SH, Saldiva PH and Rossoni LV: Endothelial dysfunction in the pulmonary artery induced by concentrated fine particulate matter exposure is associated with local but not systemic inflammation. Toxicology 295: 39-46, 2012.
4. Miller MR, Shaw CA and Langrish JP: From particles to patients: Oxidative stress and the cardiovascular effects of air pollution. Future Cardiol 8: 577-602, 2012.
5. Brown DM, Donaldson K, Borm PJ, Schins RP, Dehnhardt M, Gilmour P, Jimenez LA and Stone V: Calcium and ROS-mediated activation of transcription factors and TNF-alpha cytokine gene expression in macrophages exposed to ultrafine particles. Am J Physiol Lung Cell Mol Physiol 286: L344-L353, 2004.
6. Liu K, Hua S and Song L: PM2.5 exposure and asthma development: The key role of oxidative stress. Oxid Med Cell Longev 2022: 3618806, 2022.
7. Kim MH, Bae CH, Choi YS, Na HG, Song SY and Kim YD: Endoplasmic reticulum stress induces MUC5AC and MUC5B expression in human nasal airway epithelial cells. Clin Exp Otorhinolaryngol 12: 181-189, 2019.
8. Park SH, Gong JH, Choi YJ, Kang MK, Kim YH and Kang YH: Kaempferol inhibits endoplasmic reticulum stress-associated mucus hypersecretion in airway epithelial cells and ovalbumin-sensitized mice. PLos One 10: e143526, 2015.
9. Martino MB, Jones L, Brighton B, Ehre C, Abdulah L, Davis CW, Ron D, O'Neal WK and Ribeiro CMP: The ER stress transducer IRE1β is required for airway epithelial mucin production. Mucosal Immunol 6: 639-654, 2013.
10. Urano F, Wang X, Bertolotti A, Zhang Y, Chung P, Harding HP and Ron D: Coupling of stress in the ER to activation of JNK protein kinases by transmembrane protein kinase IRE1. Science 287: 664-666, 2000.
11. Hetz C: The unfolded protein response: Controlling cell fate decisions under ER stress and beyond. Nat Rev Mol Cell Bio 13: 89-102, 2012.
12. Keestra-Gounder AM, Byndloss MX, Seyffert N, Young BM, Chávez-Arroyo A, Tsai AY, Cevallos SA, Winter MG, Pham OH, Tiffany CR, *et al*: NOD1 and NOD2 signalling links ER stress with inflammation. Nature 532: 394-397, 2016.
13. Xu X, Li Q, Li L, Zeng M, Zhou X and Cheng Z: Endoplasmic reticulum stress/XBP1 promotes airway mucin secretion under the influence of neutrophil elastase. Int J Mol Med 47: 81, 2021.
14. Dai Y, Wang Y, Lu S, Deng X, Niu X, Guo Z, Qian R, Zhou M and Peng X: Autophagy attenuates particulate matter 2.5-induced damage in HaCaT cells. Ann Transl Med 9: 978, 2021.
15. Iordache C and Duszyk M: Sodium 4-phenylbutyrate upregulates ENaC and sodium absorption in T84 cells. Exp Cell Res 313: 305-311, 2007.
16. Yan C, Zhang L, Lu B, Lyu D, Chen H, Song F, Wang X, Chen Z, Fu Q and Yao K: Trans, trans-2,4-decadienal (tt-DDE), a composition of cooking oil fumes, induces oxidative stress and endoplasmic reticulum stress in human corneal epithelial cells. Toxicol In Vitro 68: 104933, 2020.
17. Kubra K, Akhter MS, Saini Y, Kousoulas KG and Barabutis N: Activating transcription factor 6 protects against endothelial barrier dysfunction. Cell Signal 99: 110432, 2022.
18. Pinto AR, Américo MF, Terenzi H and Silveira DB: Inhibiting IRE-1 RNase signaling decreases HIV-1 Tat-induced inflammatory M1 state in microglial cells. Biochim Biophys Acta Gen Subj 1866: 130219, 2022.
19. Porcherie A, Cunha P, Trotereau A, Roussel P, Gilbert FB, Rainard P and Germon P: Repertoire of Escherichia coli agonists sensed by innate immunity receptors of the bovine udder and mammary epithelial cells. Vet Res 43: 14, 2012.
20. Scherbakov AM, Vorontsova SK, Khamidullina AI, Mrdjanovic J, Andreeva OE, Bogdanov FB, Salnikova DI, Jurisic V, Zavarzin IV and Shirinian VZ: Novel pentacyclic derivatives and benzylidenes of the progesterone series cause anti-estrogenic and antiproliferative effects and induce apoptosis in breast cancer cells. Invest New Drug 41: 142-152, 2023.
21. Jurisic V, Srdic-Rajic T, Konjevic G, Bogdanovic G and Colic M: TNF-α induced apoptosis is accompanied with rapid CD30 and slower CD45 shedding from K-562 cells. J Membr Biol 239: 115-122, 2011.
22. Jurisic V: Multiomic analysis of cytokines in immuno-oncology. Expert Rev Proteomic 17: 663-674, 2020.
23. Livak KJ and Schmittgen TD: Analysis of relative gene expression data using real-time quantitative PCR and the 2(-Delta Delta C(T)) method. Methods 25: 402-408, 2001.
24. Hetz C, Zhang K and Kaufman RJ: Mechanisms, regulation and functions of the unfolded protein response. Nat Rev Mol Cell Bio 21: 421-438, 2020.
25. Cui X, Zhang Y, Lu Y and Xiang M: ROS and endoplasmic reticulum stress in pulmonary disease. Front Pharmacol 13: 879204, 2022.
26. Wang Z, Yao N, Fu X, Wei L, Ding M, Pang Y, Liu D, Ren Y and Guo M: Butylphthalide ameliorates airway inflammation and mucus hypersecretion via NF-κB in a murine asthma model. Int Immunopharmacol 76: 105873, 2019.
27. Ma B, Athari SS, Nasab EM and Zhao L: PI3K/AKT/mTOR and TLR4/MyD88/NF-κB signaling inhibitors attenuate pathological mechanisms of allergic asthma. Inflammation 44: 1895-1907, 2021.
28. Jurisic V, Radenkovic S and Konjevic G: The actual role of LDH as tumor marker, biochemical and clinical aspects. Adv Exp Med Biol 867: 115-124, 2015.
29. Jurisic V, Terzic T, Colic S and Jurisic M: The concentration of TNF-alpha correlate with number of inflammatory cells and degree of vascularization in radicular cysts. Oral Dis 14: 600-605, 2008.

30. Shi Y, Ji Y, Sun H, Hui F, Hu J, Wu Y, Fang J, Lin H, Wang J, Duan H and Lanza M: Nanoscale characterization of PM2.5 airborne pollutants reveals high adhesiveness and aggregation capability of soot particles. Sci Rep 5: 11232, 2015.
31. Marshall J: PM 2.5. Proc Natl Acad Sci USA 110: 8756, 2013.
32. Cao SS, Luo KL and Shi L: Endoplasmic reticulum stress interacts with inflammation in human diseases. J Cell Physiol 231: 288-294, 2016.
33. Hasnain SZ, Lourie R, Das I, Chen AC and McGuckin MA: The interplay between endoplasmic reticulum stress and inflammation. Immunol Cell Biol 90: 260-270, 2012.
34. Walter P and Ron D: The unfolded protein response: From stress pathway to homeostatic regulation. Science 334: 1081-1086, 2011.
35. Wei J, Rahman S, Ayaub EA, Dickhout JG and Ask K: Protein misfolding and endoplasmic reticulum stress in chronic lung disease. Chest 143: 1098-1105, 2013.
36. Molagoda IMN, Kavinda MHD, Choi YH, Lee H, Kang CH, Lee MH, Lee CM and Kim GY: Fisetin protects HaCaT human keratinocytes from fine particulate matter (PM2.5)-induced oxidative stress and apoptosis by inhibiting the endoplasmic reticulum stress response. Antioxidants (Basel) 10: 1492, 2021.
37. Kim SR, Kim HJ, Kim DI, Lee KB, Park HJ, Jeong JS, Cho SH and Lee YC: Blockade of interplay between IL-17A and endoplasmic reticulum stress attenuates LPS-induced lung injury. Theranostics 5: 1343-1362, 2015.
38. Schroeder BW, Verhaeghe C, Park S, Nguyenvu LT, Huang X, Zhen G and Erle DJ: AGR2 is induced in asthma and promotes allergen-induced mucin overproduction. Am J Respir Cell Mol Biol 47: 178-185, 2012.
39. Wang X, Yang X, Li Y, Wang X, Zhang Y, Dai X, Niu B, Wu J, Yuan X, Xiong A, et al: Lyn kinase represses mucus hypersecretion by regulating IL-13-induced endoplasmic reticulum stress in asthma. EBioMedicine 15: 137-149, 2017.
40. Ron D and Walter P: Signal integration in the endoplasmic reticulum unfolded protein response. Nat Rev Mol Cell Biol 8: 519-529, 2007.
41. Mijošek V, Lasitschka F, Warth A, Zabeck H, Dalpke AH and Weitnauer M: Endoplasmic reticulum stress is a danger signal promoting innate inflammatory responses in bronchial epithelial cells. J Innate Immun 8: 464-478, 2016.
42. Delmotte P and Sieck GC: Interaction between endoplasmic/sarcoplasmic reticulum stress (ER/SR stress), mitochondrial signaling and Ca(2+) regulation in airway smooth muscle (ASM). Can J Physiol Pharmacol 93: 97-110, 2015.
43. Almanza A, Carlesso A, Chintha C, Creedican S, Doultsinos D, Leuzzi B, Luís A, McCarthy N, Montibeller L, More S, et al: Endoplasmic reticulum stress signalling - from basic mechanisms to clinical applications. FEBS J 286: 241-278, 2019.
44. Laing S, Wang G, Briazova T, Zhang C, Wang A, Zheng Z, Gow A, Chen AF, Rajagopalan S, Chen LC, et al: Airborne particulate matter selectively activates endoplasmic reticulum stress response in the lung and liver tissues. Am J Physiol Cell Ph 299: C736-C749, 2010.
45. Urano F, Bertolotti A and Ron D: IRE1 and efferent signaling from the endoplasmic reticulum. J Cell Sci 21: 3697-3702, 2000.
46. Duan Q, Zhou Y and Yang D: Endoplasmic reticulum stress in airway hyperresponsiveness. Biomed Pharmacother 149: 112904, 2022.
47. Duvigneau JC, Luís A, Gorman AM, Samali A, Kaltenecker D, Moriggl R and Kozlov AV: Crosstalk between inflammatory mediators and endoplasmic reticulum stress in liver diseases. Cytokine 124: 154577, 2019.
48. Lei Y, Wang S, Ren B, Wang J, Chen J, Lu J, Zhan S, Fu Y, Huang L and Tan J: CHOP favors endoplasmic reticulum stress-induced apoptosis in hepatocellular carcinoma cells via inhibition of autophagy. PLoS One 12: e183680, 2017.
49. Kropski JA and Blackwell TS: Endoplasmic reticulum stress in the pathogenesis of fibrotic disease. J Clin Invest 128: 64-73, 2018.
50. Siddesha JM, Nakada EM, Mihavics BR, Hoffman SM, Rattu GK, Chamberlain N, Cahoon JM, Lahue KG, Daphtary N, Aliyeva M, et al: Effect of a chemical chaperone, tauroursodeoxycholic acid, on HDM-induced allergic airway disease. Am J Physiol Lung Cell Mol Physiol 310: L1243-L1259, 2016.
51. Aghapour M, Ubags ND, Bruder D, Hiemstra PS, Sidhaye V, Rezaee F and Heijink IH: Role of air pollutants in airway epithelial barrier dysfunction in asthma and COPD. Eur Respir Rev 31: 210112, 2022.
52. Gon Y and Hashimoto S: Role of airway epithelial barrier dysfunction in pathogenesis of asthma. Allergol Int 67: 12-17, 2018.
53. Bradley KL, Stokes CA, Marciniak SJ, Parker LC and Condliffe AM: Role of unfolded proteins in lung disease. Thorax 76: 92-99, 2021.
54. Byndloss MX, Keestra-Gounder AM, Bäumler AJ and Tsolis RM: NOD1 and NOD2: New functions linking endoplasmic reticulum stress and inflammation. DNA Cell Biol 35: 311-313, 2016.